SCIENCE CHINA
Technological Sciences

March 2011 Vol.54 No.3: 556–564
doi: 10.1007/s11431-010-4278-8

Fracture analysis of rock mass based on 3-D nonlinear Finite Element Method

LIU YaoRu*, CHANG Qiang, YANG Qiang, WANG ChuanQi & GUAN FuHai

State Key Laboratory of Hydroscience and Hydraulic Engineering, Tsinghua University, Beijing 100084, China

Received September 26, 2010; accepted December 16, 2010; published online January 27, 2011

Traditional fracture analysis is based on fracture mechanics and damage mechanics. They focus on the propagation of the fracture. However, their propagation criterions are not easily applied in practice and the current analysis is limited in planar problem. This paper presents a new theory that the occurrence of the unbalanced force (derived from the Deformation Reinforcement Theory) could be the criterion of the initiation of the fracture, and the distribution area and propagation of the unbalanced force could be the indication of the fracture propagation direction. By aggregate analysis with Stress Intensity Factor (SIF) criterion, the unbalanced force actually is the opposite external load that is the SIF difference incurred between the external loads and permitted by the structure. Numerical simulation and physical experiments on pre-fracture cuboid rock specimens proved that the occurrence of the unbalanced force could be the initiation of the fracture. Mesh size dependence was also considered by analysis of different mesh size finite element gravity dam models. Furthermore, the theory was applied to the feasibility analysis of the Baihetan arch dam together with physical experiments in order to evaluate the fracture propagation of dam heel. The results show that it is an effective way to use unbalanced force to analyze the fracture initiation and propagation when performing 3-dimensional nonlinear FEM calculation.

fracture analysis, rock mass, unbalanced force, plastic complementary energy norm, nonlinear finite element method

Citation: Liu Y R, Chang Q, Yang Q, et al. Fracture analysis of rock mass based on 3-D nonlinear Finite Element Method. Sci China Tech Sci, 2011, 54: 556–564, doi: 10.1007/s11431-010-4278-8

1 Introduction

Both the rock and concrete are heterogeneous and anisotropic brittle materials. Their fracturing process has close ties with the deformation and failure. Currently the fracture analysis on rock structure includes two methods: fracture mechanics [1] and continuum damage mechanics [2]. The numerical tools include Finite Element Method (FEM) [3, 4], eXtended FEM [5, 6], Element Free Method [7, 8], Boundary Element Method [9], Discrete Element Method [10], Numerical Manifold Method [11], Lattice model [12] and etc.

There are two methods in the fracture propagation simulation: Smeared Fracture Model [13] and Discrete Fracture Model [14]. For the first one, the fracture was simulated by parallel and serried elements. For the second one, the workload for remesh is heavy when separating the grid in order to simulate the fracture. What is worse, the mapping method of the new variables has not been resolved yet [15, 16]. Fracture mechanics and damage mechanics analyses were combined by some researchers [17]. This combined approach unites the accuracy of the special fracture-tip elements in fracture mechanics with the flexibility of fracture representation in damage mechanics and is an effective means for the analysis of fracture propagation by the Finite Element Method.

For the initiation and propagation of the fracture, there are several criterions: maximum tensile stress criterion [18],

*Corresponding author (email: liuyaoru@tsinghua.edu.cn)

Stress Intensity Factor (SIF) criterion [1], maximum energy release rate criterion [19, 20], minimum strain energy density criterion [21–23]. SIF criterion and maximum energy release rate criterion are mathematically equivalent. Rice proposed J-integral (together with Crack Opening Displacement, COD) to determine whether the fracture tip began to extend [1].

Those solutions mentioned above are effective in the planar analysis. However, the calculation workload is heavy, and the criterion is still outstanding when extended to 3-dimensional structure. Besides, the numerical methods used now are mainly based on linear plastic, while the actual rock and concrete are nonlinear materials. This paper presents a new theory that the occurrence of unbalanced force (derived from the Deformation Reinforcement Theory (DRT)) [24, 25] could be the criterion of the initiation of fracture, and the distribution area and propagation could be the indication of the fracture propagation direction. Numerical simulation and physical experiments on pre-fracture cuboid rock specimens proved that the occurrence of unbalanced force could be the initiation of the fracture. Mesh size dependence was also considered by analysis of different mesh size finite element dam models. Furthermore, the theory was applied to the feasibility analysis of the Baihetan arch dam together with physical experiments in order to evaluate the fracture propagation.

2 Fracture analysis based on Deformation Reinforcement Theory

2.1 Deformation Reinforcement Theory

The rock and concrete are nonlinear materials, and currently the numerical analysis on those structures is mainly based on elastoplasticity. Solutions of elastic structures always exist and are unique, but solutions of elasto-plastic structures may not exist. The existence of structural solutions implies that the displacement and stress fields throughout the structure satisfy simultaneously equilibrium condition, kinematical admissibility and constitutive equations including yield conditions under prescribed loading, so the structure is stable. The constitutive equations contain the yield criterion. If the structure could not maintain stable, there is no solution that could satisfy simultaneously the three conditions mentioned above.

Considering the arbitrary kinematical and equilibrium stress-field, $\boldsymbol{\sigma}_1$, and kinematical and stable stress-field, $\boldsymbol{\sigma}$, their difference is the plastic-stress increment field $\Delta\boldsymbol{\sigma}^{\mathrm{p}}$:

$$\Delta\boldsymbol{\sigma}^{\mathrm{p}} = \boldsymbol{\sigma}_1 - \boldsymbol{\sigma} . \tag{1}$$

The plastic-stress increment field $\Delta\boldsymbol{\sigma}^{\mathrm{p}}$ leads to the plastic-strain increment field $\Delta\boldsymbol{\varepsilon}^{\mathrm{p}}=C\colon \Delta\boldsymbol{\sigma}^{\mathrm{p}}$, while $\boldsymbol{C}$ is the fourth-order compliance tensors.

Define a Euclidean space about stress field, and an arbitrary stress field is a point in the Euclidean space. Suppose a structure whose volume is V, if metric tensor is $\boldsymbol{C}/2$, plastic complementary energy can be defined as

$$\Delta E = \frac{1}{2}\int_V \Delta\boldsymbol{\sigma}^{\mathrm{p}} : \boldsymbol{C} : \Delta\boldsymbol{\sigma}^{\mathrm{p}} \mathrm{d}V . \tag{2}$$

This equation shows that ΔE is also the norm of plastic-stress increment field $\Delta\boldsymbol{\sigma}^{\mathrm{p}}$. If $\Delta E=0$, then $\Delta\boldsymbol{\sigma}^{\mathrm{p}}$ is always zero and the structure is stable. If $\Delta E>0$, the structure is unstable.

Since stress field $\boldsymbol{\sigma}_1= \boldsymbol{\sigma}+ \Delta\boldsymbol{\sigma}^{\mathrm{p}} = [\,\sigma^1_{ij}]$ is a kinematical and equilibrium stress-field, it satisfies equilibrium condition. Assume that the body-force field is $\boldsymbol{f}=\{f_i\}$ loading on an elasto-plastic structure, and S_σ is stress boundary with $\boldsymbol{T}= T_i = \{\sigma_{ij}n_j\}$. For an arbitrarily given virtual displacement $\delta\boldsymbol{u}=\{\,\delta u_i\}$, the corresponding virtual strain is $\delta\varepsilon_{ij}$. So the principle of virtual displacements reads

$$\int_V \delta\varepsilon_{ij}\sigma^1_{ij}\mathrm{d}V = \int_V \delta u_i f_i \mathrm{d}V + \int_{S_\sigma} \delta u_i T_i \mathrm{d}S , \tag{3}$$

that is

$$\int_V \delta\varepsilon_{ij}\sigma_{ij}\mathrm{d}V = \int_V \delta u_i f_i \mathrm{d}V + \int_{S_\sigma} \delta u_i T_i \mathrm{d}S - \int_V \delta\varepsilon_{ij}\Delta\sigma^{\mathrm{p}}_{ij}\mathrm{d}V . \tag{4}$$

Assume $\boldsymbol{N}$ is shape function matrix, $\boldsymbol{B}$ is strain matrix, $\boldsymbol{F}$ is equivalent nodal force vector of external loads. Then the governing equation of FEM can be deduced from the principle of virtual displacements

$$\sum_e \int_{Ve} \boldsymbol{B}^{\mathrm{T}}\boldsymbol{\sigma}_1 \mathrm{d}V = \sum_e \int_{Ve} \boldsymbol{N}^{\mathrm{T}}\boldsymbol{f}\mathrm{d}V + \sum_e \int_{S^e_\sigma} \boldsymbol{N}^{\mathrm{T}}\boldsymbol{T}\mathrm{d}S , \tag{5}$$

that is

$$\sum_e \int_{Ve} \boldsymbol{B}^{\mathrm{T}}\boldsymbol{\sigma}\mathrm{d}V = \boldsymbol{F} - \sum_e \int_{Ve} \boldsymbol{B}^{\mathrm{T}}\Delta\boldsymbol{\sigma}^{\mathrm{p}}\mathrm{d}V = \boldsymbol{F} - \Delta\boldsymbol{Q} , \tag{6}$$

where $\Delta\boldsymbol{Q}$ is the equivalent nodal force to plastic-stress increment field $\Delta\boldsymbol{\sigma}^{\mathrm{p}}$ which is called unbalanced forces in FEM:

$$\Delta\boldsymbol{Q} = \sum_e \int_{Ve} \boldsymbol{B}^{\mathrm{T}}\Delta\boldsymbol{\sigma}^{\mathrm{p}}\mathrm{d}V , \tag{7}$$

where $\Delta\boldsymbol{Q}$ indicates the extent beyond the yield surface.

2.2 Fracture analysis on rock

The unbalanced force can be used as the measurement of the unstability of the rock. The structure is unstable if there is unbalanced force in some area under the prescribed loads. So the unbalanced force can be used to evaluate the fracturing of rock.

(1) The initiation and propagation of the fracture

The amount of unbalanced force incurred by external load represents the extent of the fracture propagation. The development of the unbalanced force is the process of the propagation of the fracture.

(2) Determination of fracture location

The unbalanced forces are self-balanced. The area where unbalanced forces occur is the location where the fracture initiates.

2.3 Criterion of the fracture propagation

The 3-D mechanical status of the fracture area is complicated. Consequently the analysis is mainly on 2-D elasto-plastic currently. The discussion of this section is also for 2-D. As the conditions were not limited for 2-D, the result of the discussion is also applicable to 3-D.

In the traditional theory of elasto-plastic fracture mechanics, the energy released by fracture propagation is provided for the newly formed surface. When the energy released G is more than double surface energy T, the fracture extends. In another word, the fracture criterion is $G = G_c$. The relationship between SIF and energy release rate is as follows [1]:

$$G = \frac{K_{\mathrm{I}}^2 + K_{\mathrm{II}}^2}{E} + \frac{K_{\mathrm{III}}^2}{2\nu}, \tag{8}$$

where K_{I}, K_{II} and K_{III} are Stress Intensity Factor for mode-I, mode-II and mode-III respectively.

$G = G_c$ could be rewritten as $K = K_c$, where K_c is the limit of SIF. In fact, the SIF criterion and maximum energy release rate criterion are mathematically equivalent. Besides, the SIF criterion is applied successfully to the large region yield status analysis.

It is difficult to calculate SIF when performing the FEM analysis. For example, suppose FEM is used to analyze the structure described in Figure 1, and the calculation is satisfactorily approximate. When the loads $\sigma < \sigma_c$, $K < K_c$, the fracture does not extend. When $\sigma < \sigma_c$, $K < K_c$, the fracture is in the critical state and the mechanical solution of the entire structure is still available. When $\sigma < \sigma_c$, $K < K_c$, the fracture extends, and the mechanical solution does not exist. There are new surfaces generated. At this time, external forces F^* were required in order to restrict the propagation of fracture. That means if SIF incurred by F^* meets the condition $K^* < K_c - K$, rewritten as $K^* + K < K_c$, the fracture will not extend. F^* represents the unbalanced force derived from the elasto-plastic FEM calculation.

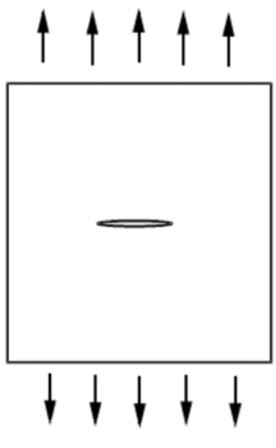

Figure 1 Typical loading conditions of fracture.

For traditional FEM, the iteration does not converge when $K < K_c$ as the FE topological structure does not change. Consequently the unbalanced force is incurred. The force opposite to the unbalanced force could maintain the structure stable together with external loads. In other words, if ΔQ represents the unbalanced force, and F is external loads, the equation can be rewritten as

$$K_{-\Delta Q} + K_F = K_c, \tag{9}$$

where $K_{-\Delta Q}$ and K_F are SIF under $-\Delta Q$ and F respectively.

That is, the composition of SIF incurred by external loads and the force opposite to the unbalanced force is equal to the permitted SIF. When $K \leqslant K_c$, $\Delta Q = 0$. The iteration of FEM is the process of seeking the minimum additional forces in order to restrict the propagation of fracture. These additional forces can be 0 or not. Further more, if the unbalanced force is close to 0 after iteration in elasto-plastic FEM calculation, the fracture will not propagate or in the critical state. While if the unbalanced force cannot be iterated to 0, the fracture will extend. As there is actually no additional unbalanced force in physical structure, the structure will fail in the area where unbalanced force occurs. That means the fracture extends through the unbalanced area. So the unbalanced force can be used to determine when and where the fracture extends.

3 Numerical and physical experiments on precrack rock specimens

3.1 Cuboid rock specimen with single precrack

Cuboid rock specimen with single precrack [21] (shown in Figure 2) was made of granite of 40 mm×20 mm×8 mm). The precrack was incised by ultrasound drill (1 mm), and then filled with the granite powder mixed with acrylate bond. α represents the angle between the precrack and the pressure-bearing surface. Its value is 15°, 30°, 45°, 60°, 75°, 90° respectively. The length of precrack was fixed as 4 mm.

The result of physical experiments was illustrated in Figure 3 [26]. When α was small, the crack extended smoothly before failure, and the start cracking pressure level was high. When α was larger than 60°, though the start cracking pressure level was low, the crack extended dramatically when the pressure was close to the upper limit, then the specimen failed suddenly.

The finite element numerical meshes were generated according to the physical specimens. The unbalanced force vector graphs were illustrated in Figure 4. The result is as follows:

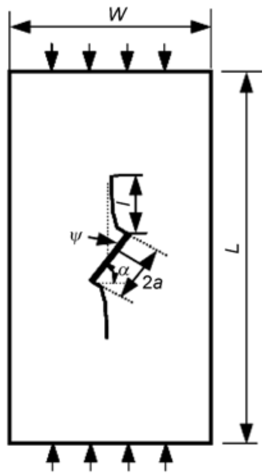

Figure 2 Cuboid rock specimen with single precrack.

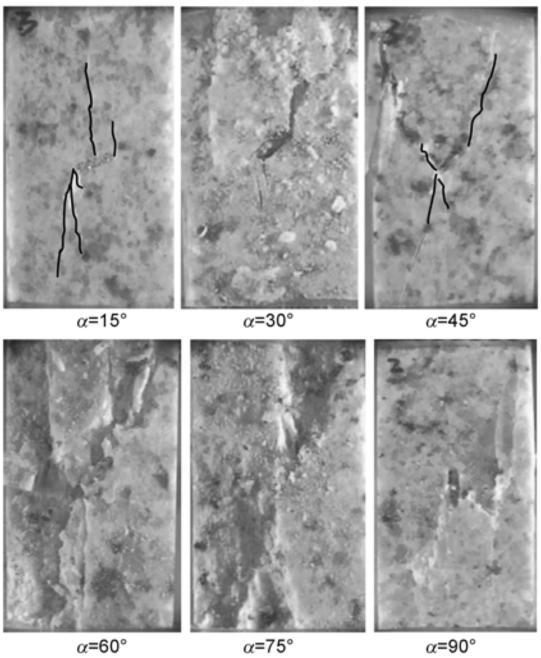

Figure 3 Physical experiment result for single precrack cuboid [26].

(1) The unbalanced force firstly occurred in the precrack's tips, its direction was not along the precrack direction, but almost perpendicular to the precrack. The result was proved by physical experiments.

(2) As the external loads increased, the crack began to extend, and its direction gradually tended to the direction of principal compressive stress, the same as the actual failure model illustrated in Figure 3.

(3) The directions of crack extension may be perpendicular to the precrack. α =15° and 45° in Figure 4 described these situations.

3.2 Cuboid rock specimen with double precracks

The physical model of double precracks cuboid rock speci-

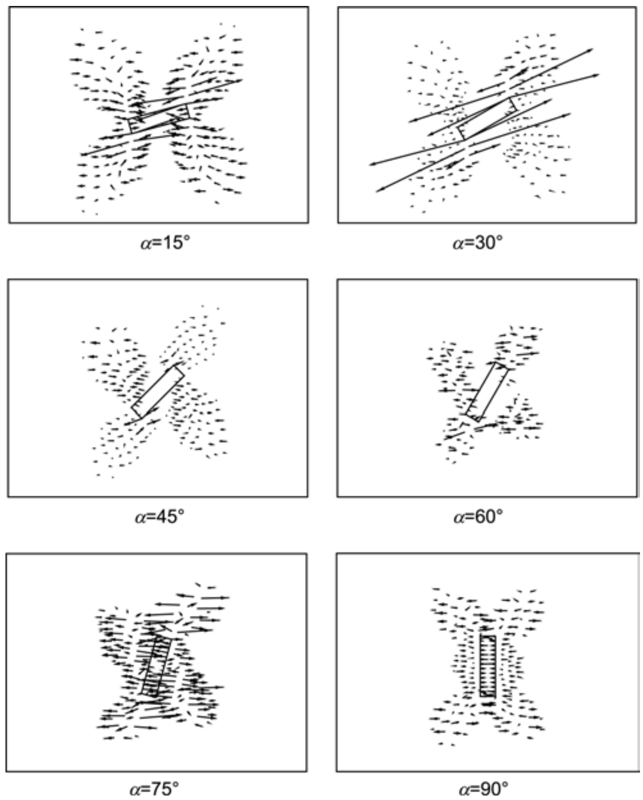

Figure 4 Unbalanced force vector results of single precrack cuboid.

men is illustrated in Figure 5. The length of the crack is still fixed as 4 mm. ① and ② represent the precracks. Their angles were kept as 45°. The rock bridge angle β increased from 75° to 120° (15° per step). Figure 6 shows the different finite element mesh models.

The physical experiment results are illustrated in Figure 7 [26]. Initially the wing cracks occurred in both of the outer and inner tip areas of the precracks. The outer wing crack extended through a direction with an angle to the precrack. At the same time, the inner crack penetrated through different

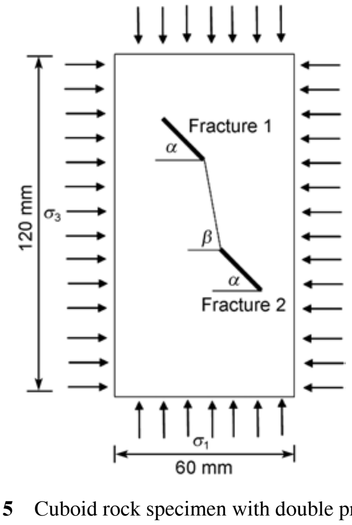

Figure 5 Cuboid rock specimen with double precracks.

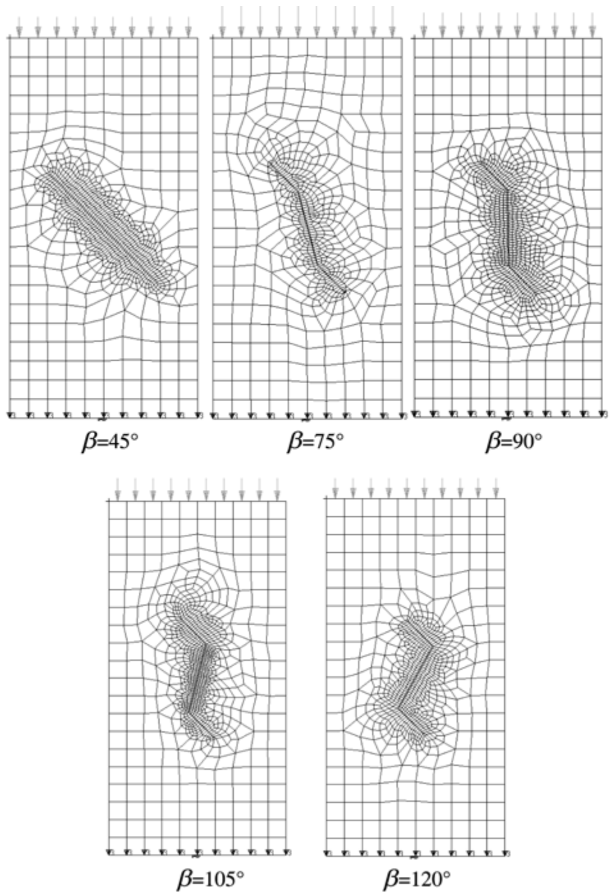

Figure 6 Finite element model of the double precracks cuboid.

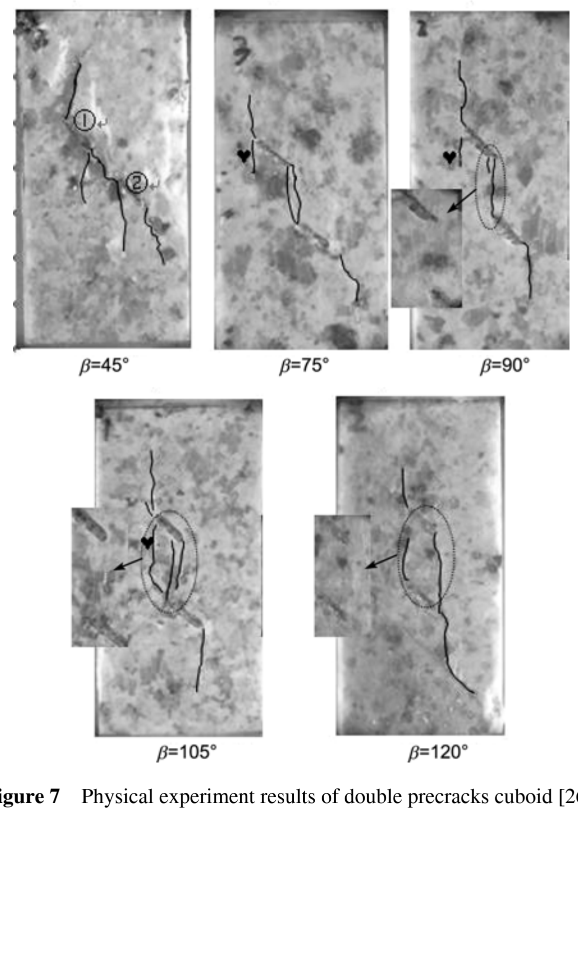

Figure 7 Physical experiment results of double precracks cuboid [26].

ways. That is, the inner crack generated from precrack ① extended to the inner crack generated from precrack ②.

Figure 8 shows the unbalanced force vector distributions for different finite element models. From the comparison between Figures 7 and 8, it is reasonable to use the unbalanced force direction as the propagation direction of the crack.

4 Mesh size dependence analysis

The microscopic characteristics of the structure (strain softening, localization and mesh dependence and etc.) have a significant influence on the ultimate failure mode. However, to decrease excessively the size of mesh is not an effective way in finite element analysis. When the mesh size is decreased to typical scale of the rock and concrete, the property parameters are meaningless. What is worse, the tensile stress gets larger and larger when the mesh size is decreased in stress singularity area. That affects quite an area of finite element model.

To analyze the mesh size dependence of the unbalanced force, we built the dam heel model illustrated in Figure 9. The bottom side was fixed, and the upper and downstream boundaries were normally fixed. Five different sizes of mesh were generated around the area of the dam heel (40 m ×40 m). Figure 10 showed the mesh whose sizes were 3, 2.5, 2, 1.5, 1.0, 0.5 m respectively. The external load was water pressure from the upper stream.

The unbalanced force vector graphs corresponding to different mesh sizes were illustrated in Figure 11. As the mesh size got smaller, the arrows of the unbalanced force

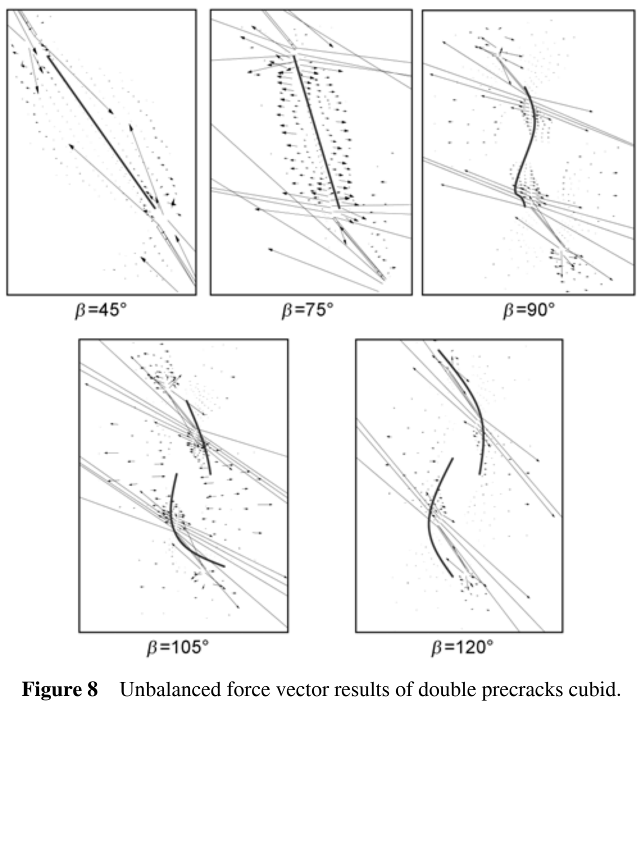

Figure 8 Unbalanced force vector results of double precracks cubid.

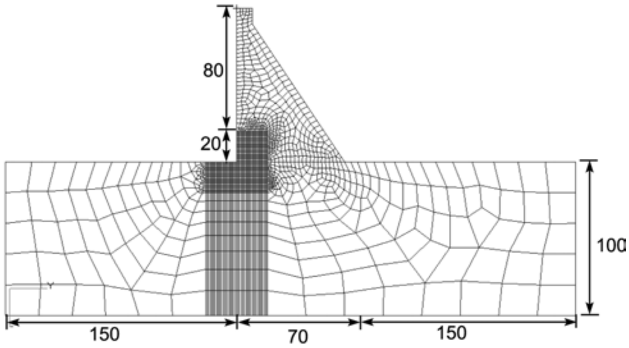

Figure 9 Finite element model of dam heel (m).

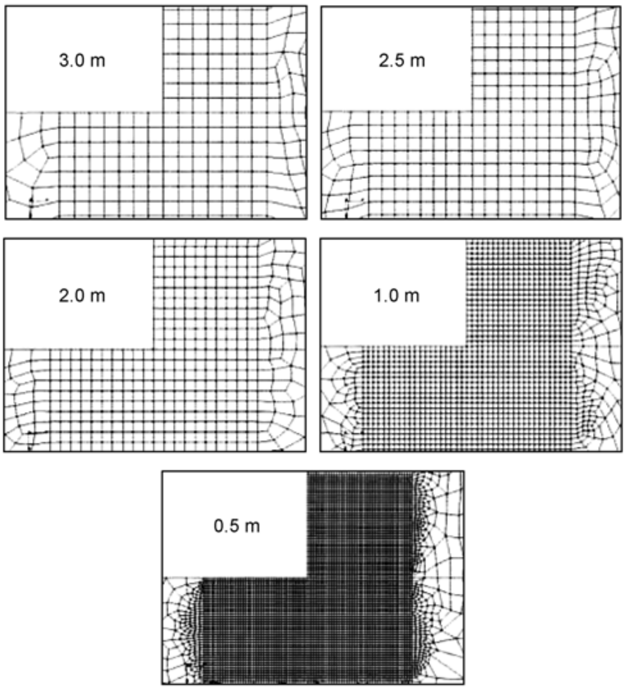

Figure 10 Different mesh size finite element models of dam heel.

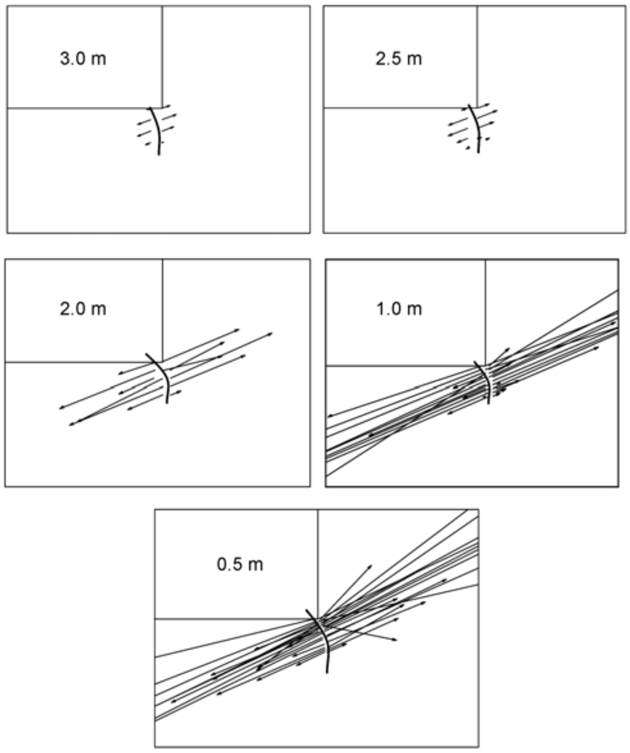

Figure 11 Unbalanced force vector results for different mesh sizes.

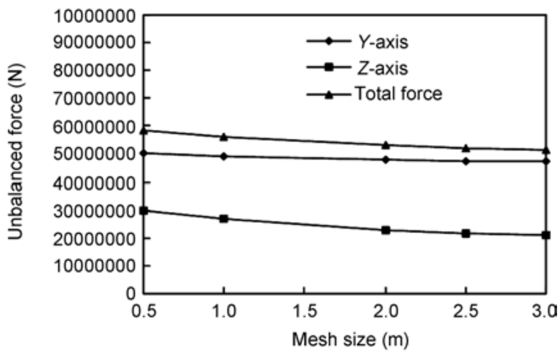

Figure 12 Unbalanced force magnitude results for different mesh sizes.

got longer and concentrated, while the distribution areas were kept unchanged. As a result, it was reasonable to use the distribution of the unbalanced force as the crack propagation direction.

Figure 12 illustrated the *Y* (along the stream), *Z* (perpendicular to the stream) directions and total unbalanced force magnitude corresponding to the different mesh sizes. When the mesh sizes decreased from 3 m (3% of the dam height) to 0.5 m (0.5% of the dam height), the unbalanced force magnitude of *Y* and *Z* directions increased by 6.4% and 41.7% respectively, the total amount increased by 13.1% as the mesh sizes decreased 6 times.

Figure 13 illustrated the plastic complementary energy norm (PCE, which describes the stability of the structure [24]) curves corresponding to the different mesh sizes. PCE norm was kept steady (0) before occurring (when the external water pressure was 2.5 times to the benchmark), but varied after that.

From the discussion above, we could conclude that the magnitude of the unbalanced force in the dam heel area is not significantly influenced by the mesh sizes. The unbalanced force concentrated in the dam heel area, and its distribution in other area is comparatively less except for stress concentration area (rock faults, dam heel etc.). As a result, the magnitude of the unbalanced force can be obtained by just summarizing the value of the dam heel area instead of specifying until the total amount is close to 0. Then the positive (or negative) amount is the unbalanced force magnitude.

Besides, though the PCE norm varies corresponding to the mesh size of the dam heel after occurrence, the catastrophe point keeps stable. It could be used as the criterion of

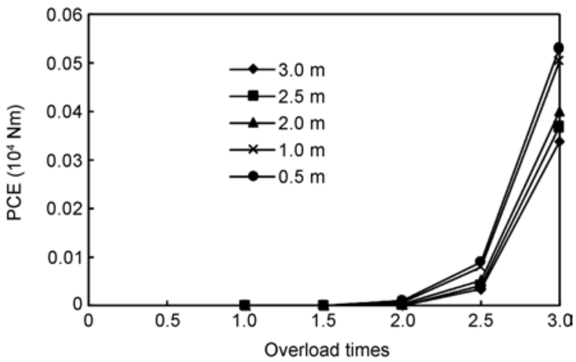

Figure 13 The PCE norm curve for different mesh sizes.

the stability.

5 Fracture analysis of dam heel of Baihetan arch dam

Baihetan hydropower station located in Sichuan Province, China, the downstream area of Jinsha River. The height of arch dam is 289 m. The valley is asymmetrical "V"-shaped. Its left bank is gentle and right bank is steep, as shown in Figure 14. Both the 3-D finite element numerical and physical experiments were performed. The finite element model size is as follows:

- Upper stream: 1.5 times of the height of dam (500 m);
- Down stream: 2.5 times of the height of dam (700 m);
- Left and right banks: 3 times of the height of dam (800 m each);
- Height above the dam: 50 m;
- Height beneath the dam: 324 m.

Various rock materials and faults were simulated. The finite element mesh model is shown in Figure 15.

The physical model was built in a steel frame whose size is 4.6 m×4.6m×2.8 m. The model scale is 1:250. Figures 16 and 17 are the physical arch dam model and loading device.

Figure 18 illustrated the unbalanced force contour maps of dam heel area corresponding to different water loads. When the load was normal (1.0 water pressure), the dam worked in elastic condition, no unbalanced force was incurred.

Figure 14 The environment of the dam location.

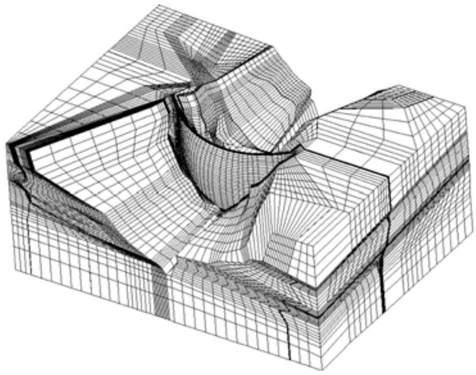

Figure 15 Numerical mesh model of Baihetan arch dam.

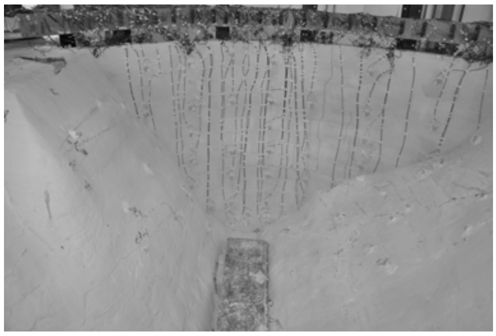

Figure 16 The physical model of arch dam.

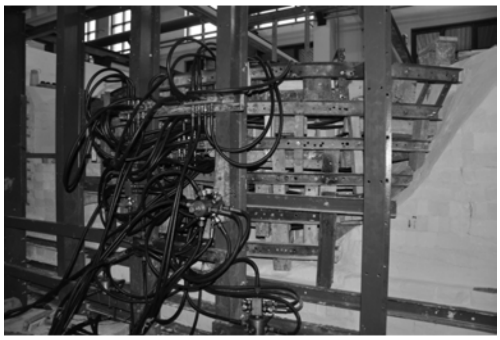

Figure 17 The loading devices.

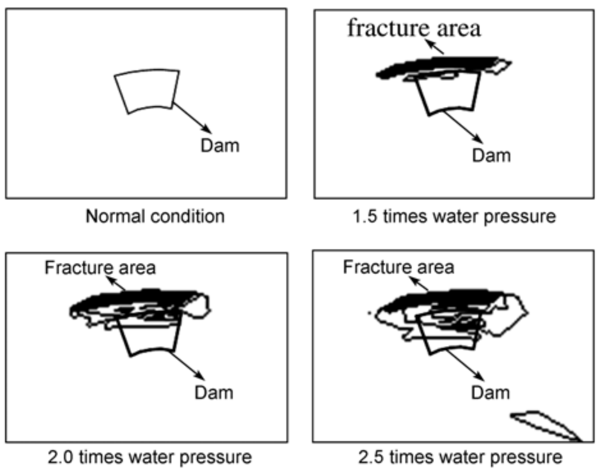

Figure 18 Photographs of the experiment platform.

As the load increased, the unbalanced force occurred, and became more in line with the loads.

The unbalanced force concentrated in the upper stream river bed area near the dam heel where there is a default crossing. When the work load was 1.5 times normal pressure, the fault worked in compressive-shear stress condition. When the work load was 2.0 times normal pressure, the fault worked in tensile-shear stress condition.

The final crack picture was shown in Figure 19. The crack propagation of the dam heel river bed area corresponding to the water loads was shown in Figure 20. There was initial crack incurred in the upper stream river bed (about 14.5 m to the dam heel) when the work load was 1.5 times water pressure, the same as the numerical results. When the work load increased to 2.5 times water pressure, the crack penetrated through the river bed.

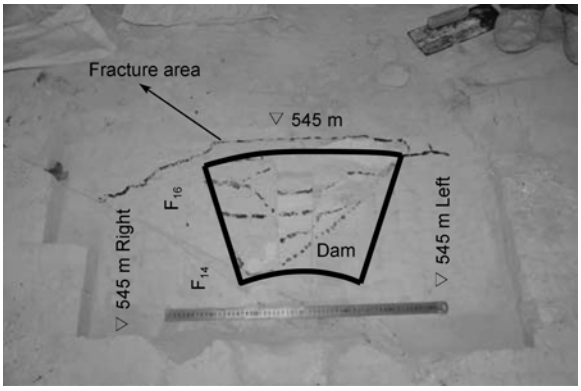

Figure 19 The final crack status of the dam heel river bed area.

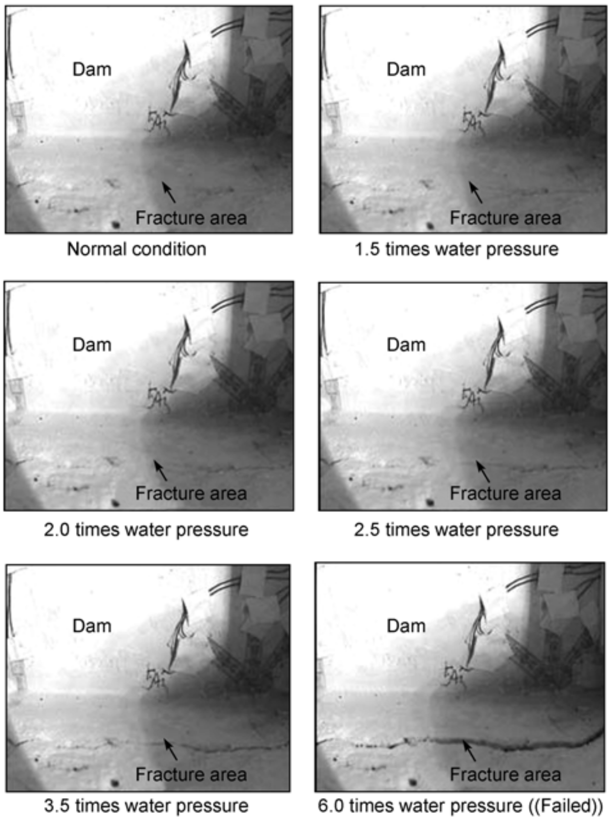

Figure 20 Crack propagation of the dam heel river bed area corresponding to the water loads.

6 Conclusion

This paper presents a new theory focused on the fracture initiation and propagation based on the unbalanced force derived from elasto-plastic finite element analysis of DRT. The area of the structure where the unbalanced force occurred is the location where the fracture may initiate. The distribution area and propagation of the unbalanced force could be the indication of the fracture propagation direction. Mesh size has little effect in fracture analysis. This theory could be implemented in the analysis of practical fracture initiation and propagation based on 3-D nonlinear finite element analysis which had been widely used in rock soil engineering. Compared with other fracture analysis method, the method in this paper does not need any extra parameters, and can avoid complex topological calculation of FEM mesh in fracture propagation analysis.

The composition of SIF incurred by external loads and unbalanced force is equal to the permitted SIF when small area of the structure yielded and the fracture began to extend. Compared with SIF incurred by external loads, the unbalanced force is the force calculated by FEM which is beyond the yield surface, as a result the theory could also be applied to large yield area. The unbalanced force and SIF incurred actually represent the propagation status of the fracture. The numerical and physical experiment results have proved that this theory could be effective in evaluating the fracture propagation.

This work was supported by the National Natural Science Foundation of China (Grant No. 50709014), China National Funds for Distinguished Young Scientists (Grant No. 50925931) and State Key Laboratory of Hydroscience and Engineering of China (Grant No. 2008-TC-2).

1 Yang W. Macro-micro Fracture Mechanics (in Chinese). Beijing: National Industry Press, 1995
2 Geersa M G D, De Borst R, Peerlings R H J. Damage and crack modeling in single-edge and double-edge notched concrete beams. Eng Fract Mech, 2000, 65: 247–261
3 Tang C A. Numerical tests of progressive failure in brittle materials (in Chinese). Mech Eng, 1999, 21(2): 21–24
4 ChenY Q, Zheng X P, Yao Z H. Explanation of strain softening and numerical modeling to the failure process of laminated composite material (in Chinese). Chin J Comput Phys, 2003, 20(1): 14–20
5 Dumstorffz P, Meschke G. Crack propagation criteria in the framework of X-FEM-based structural analyses. Int J Numer Anal Meth Geomech, 2007, 31: 239–259
6 Fang X J, Jin F, Wang J T. Simulation of mixed-mode fracture of concrete using extended finite element method (in Chinese). Eng Mech, 2007, 24(Supp I): 46–52
7 Kou X D, Zhou W Y. The application of element-free method to approximate calculation of arch dam crack propagation (in Chinese).

J Hydraul Eng, 2000, 10: 28–35
8 Huang Y S, Zhou W Y, Hu Y J. Crack propagation tracing by using 3-D element-free Galerkin method(in Chinese). J Hydraul Eng, 2006, 37(1): 63–69
9 Xiao H T, Yue Z Q. Boundary element analysis of 3D crack problems in layered materials (in Chinese). Chin J Comput Mech, 2003, 20(6): 721–724
10 Hou Y L, Zhou Y D, Zhang C H. Tensile shear mixed mode fracture analysis of concrete rock material by distinct element method (in Chinese). Chin J Comput Mech, 2007, 24(6): 773–778, 784
11 Wang S L, Ge X R. Application of manifold method in simulating crack propagation (in Chinese). Chin J Rock Mech Eng, 1997, 16(5): 319–332
12 Yang Q, Zhang H, Wu R Z. Lattice model simulation of fracture in disordered brittle materials (in Chinese). Chin J Rock Mech Eng, 2000, 19(Supp): 941–945
13 Hillerborg A, Modéer M, Peterson P E. Analysis of crack propagation and crack growth in concrete by means of fracture mechanics and finite elements. Cem Concr Res, 1976, 6: 773–782
14 Bazant Z P. Crack band model for fracture of geomaterial. In: Eisenstein Z, ed. Proc 4th Int Conf on Numerical Methods in Geomechanics, Edmonton: Univ of Alberta, 1982, 3: 1137–1152
15 Blackburn W S. A remeshing algorithm for three-dimensional crack growth and intersection with surfaces or cracks in non-coplanar planes. Eng Anal Bound Elem, 2000, 24: 343–350
16 Bouchard P O, Bay F, Chastel Y. Numerical modelling of crack propagation: automatic remeshing and comparison of different criteria. Comput Method Appl Mech Eng, 2003, 192: 3887–3908
17 Van Vroonhovena J C W, De Borst R. Combination of fracture and damage mechanics for numerical failure analysis. Int J Solids Struct, 1999, 36: 1169–1191
18 Erdogan F, Sih G C. On the crack extension in plates under plane loading and transverse shear. ASME J Basic Eng, 1963, 85(4): 519–527
19 Hussain M A, Pu S L, Underwood J. Strain energy release rate for a crack under combined mode I and mode II. In: Paris P C, Irwin G R, eds. Fracture Analysis, ASTM STP 560, 2–28, Philadelphia, PA. American Society for Testing and Materials, 1993
20 Palaniswamy K, Knauss W G. On the problem of crack extension in brittle solids under general loading. In: Nemat-Nasser S, ed. Mechanics Today, vol 4. Oxford: Pergamon Press, 1978. 87–148
21 Sih G C. Strain energy density factor applied to mixed mode crack problems. Int J Fract, 1974, 10(3): 305–321
22 Cotterell B, Rice J R. Slightly curved or kinked cracks. Int J Fract, 1980,16(2): 155–169
23 Theocaris P S, Andrianopoulos N P. The Mises elastic-plastic boundary as the core region in fracture criteria. Eng Fract Mech, 1982, 16(3): 425–432
24 Yang Q, Liu Y R, Chen Y R, et al. Deformation reinforcement theory and global stability and reinforcement of high arch dams. Chin J Rock Mech Eng (in Chinese), 2008, 27(6): 1121–1136
25 Yang Q, Chen X, Zhou W Y，et al. On unbalanced forces in 3D elastoplastic finite element analysis(in Chinese). Chin J Geotech Eng, 2004, 26(3): 323–326
26 Lin P. Brittle failure behaviour of medium containing flaws and pore (in Chinese). Doctoral Thesis. Shengyang: The Northeastern University, 2002